Third International Conference on CFD in the Minerals and Process Industries
CSIRO, Melbourne, Australia
10-12 December 2003

NUMERICAL PREDICTION OF SHEAR-THINNING DROP FORMATION

Malcolm R. DAVIDSON and Justin J. COOPER-WHITE

Department of Chemical and Biomolecular Engineering
The University of Melbourne, Victoria 3010, AUSTRALIA

ABSTRACT

A Volume-of-Fluid numerical method is used to predict the dynamics of shear-thinning liquid drop formation in air from a circular orifice. The validity of the numerical calculation is confirmed for a Newtonian liquid by comparison with experimental measurements. For particular values of Weber number and Froude number, predictions for a shear-thinning drop show an expected more rapid pinch-off, but also a minimum in the limiting drop length as the zero-shear viscosity is varied. However the dominant effect on drop length is a reduction due to shear-thinning at higher viscosities. The evolution of predicted drop shape, drop thickness and length, and the configuration at pinch-off are discussed for various shear-thinning parameters.

NOMENCLATURE

a internal radius of the nozzle
C fractional volume function
Fr Froude number $\overline{V}^2/ga$
$\mathbf{F_S}$ surface force
g gravitational acceleration
$\hat{\mathbf{g}}$ unit vector in the direction of gravity
h minimum neck thickness
L drop length below the nozzle
n shear-thinning parameter
Oh Ohnesorge number $\sqrt{\text{We}}/\text{Re}$
P pressure
Re Reynolds number $\rho_1 \overline{V} a/\mu_{10}$
t time
t_d time to pinch-off
$\mathbf{U}$ velocity
$\overline{V}$ mean inlet velocity
We Weber number $\rho_1 \overline{V}^2 a/\sigma$

$\dot{\gamma}$ dimensionless shear rate
η dimensionless Carreau viscosity μ_1/μ_{10}
η_∞ $\mu_{1\infty}/\mu_{10}$
λ shear-thinning parameter
μ viscosity
ρ density
σ surface tension
$\boldsymbol{\tau}$ stress tensor

Subscripts

1 drop phase
2 air phase
0 zero shear rate

INTRODUCTION

The growth and detachment of drops from a nozzle is a familiar occurrence (e.g. a dripping tap), which is also important in many industrial applications (e.g. ink-jet printing, biological assays). For drop formation from a nozzle under the influence of gravity when the liquid flow rate is low, the pendant drop grows slowly at first with drop shape determined by a quasi-static balance between gravity and interfacial tension. Once the drop volume reaches a critical value, force equilibrium is lost leading to the rapid development of necking and break-up (pinch-off) of the pendant drop. Eggers (1997) gives a detailed review of recent fluid dynamic research on interfacial break-up phenomena for dripping nozzles, jets, liquid bridges and other related problems. Wilkes et al. (1999) and Cooper-White et al. (2002) provide more recent summaries concerning pendant drops.

Apart from work based on a one-dimensional approximation (Eggers, 1997), numerical studies include boundary integral solutions of potential flow (Schulkes, 1994) and Stokes flow (Zhang and Stone, 1997), and finite element (Wilkes et al., 1999; Notz et al., 2001; Chen et al., 2002; Ambravaneswaran et al., 2002) and volume-of-fluid (Gueyffier et al., 1999; Zhang, 1999a,b) solutions of the full Navier-Stokes equations.

In many practical circumstances (e.g. biological fluids), the drop fluid can be non-Newtonian. The evolution of a pendant drop of visco-elastic fluid has been studied experimentally by Amarouchene et al. (2001) and more comprehensively by Cooper-White et al. (2002). Yildirim and Basaran (2001) used a finite element numerical method to examine the deformation and break-up of Newtonian and shear-thinning liquid bridges contained between two disks. Very recently, the authors (Davidson et al., 2003) demonstrated the use of a volume-of-fluid (VOF) numerical method to predict the growth and pinch-off of a pendant drop of shear-thinning liquid. Apart from this, there appears to be no published numerical study of the evolution of a pendant drop of non-Newtonian liquid. The aim of this paper is to present and discuss additional results from a continuation of the work of Davidson et al. (2003).

MODEL FORMULATON

Consider axi-symmetric evolution of a pendant drop growing downwards in air from a nozzle of internal diameter $2a$ and external diameter $4a$ as shown in Figure 1. The liquid is assumed to wet the nozzle wall so that the liquid-air interface is attached at the outer nozzle diameter.

The flow domain is taken to be a cylindrical region about the axis of symmetry with radius $4a$ (i.e. twice the outer radius of the nozzle) below the nozzle and radius a within the nozzle. The length of the flow domain is chosen to be sufficient to completely contain the drop fluid for the duration of the calculation. The drop and the surrounding air are considered to be a single fluid with variable properties. This fluid takes the properties of the liquid within the drop and those of air within the surroundings. Here the ratio of the air viscosity to the liquid viscosity at zero shear (μ_{10}) is taken to be 0.003. The corresponding density ratio is 0.001.

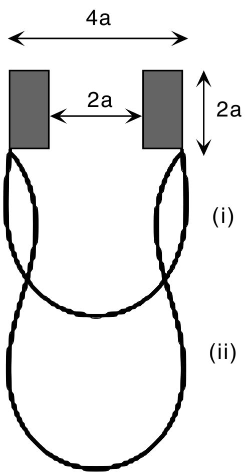

Figure 1: Schematic showing (i) the initial drop shape and (ii) the drop shape at a later time. The shaded parts indicate the annular nozzle wall.

The equations of motion, with velocity, length and time scaled according to $\bar{V}$, a and $a/\bar{V}$, respectively, are

$$\frac{\partial C}{\partial t} + \nabla \cdot (\mathbf{U}C) = 0 \tag{1}$$

$$\frac{\partial \rho \mathbf{U}}{\partial t} + \nabla \cdot (\rho \mathbf{U}\mathbf{U}) = -\nabla P + \frac{\rho \hat{\mathbf{g}}}{\mathrm{Fr}} + \frac{\mathbf{F}_s}{\mathrm{We}} + \frac{1}{\mathrm{Re}} \nabla \cdot \boldsymbol{\tau} \tag{2}$$

$$\nabla \cdot \mathbf{U} = 0 \tag{3}$$

$$\rho = \rho_1 C + \rho_2 (1 - C) \tag{4}$$

The Carreau model of shear-thinning is used for the drop fluid where the dimensionless Carreau viscosity is given by

$$\frac{\eta - \eta_\infty}{1 - \eta_\infty} = \left(1 + (\lambda \dot{\gamma})^2\right)^{\frac{1}{2}(n-1)} \tag{5}$$

The shear rate $\dot{\gamma}$ is the second invariant of the rate of strain tensor (Bird et al., 1987).

A stable equilibrium drop shape was used as an initial condition. This was determined in a pre-calculation with zero inflow at the nozzle, beginning with a specified drop volume below the nozzle (in dimensionless terms we choose $40\pi/3$, corresponding to a cylinder of radius 2 and height 2, capped at its base by a hemisphere of radius 2).

A parabolic velocity profile was chosen at the inflow to the nozzle. A linear profile, as set by Schulkes (1994) and Gueyffier et al. (1999), was also tried, yielding almost identical results. The velocity profile at inflow is also set at the bottom of the computational domain (with zero velocity when $r > a$) to conserve the total volume of fluid therein. Zero normal gradients in C are set at the domain boundaries except at the inlet to the nozzle where $C = 1$. Free slip velocity conditions are taken at radial boundary of the domain below the nozzle. The usual no-slip condition applies at the nozzle wall.

NUMERICAL CONSIDERATIONS

The VOF algorithm of Rudman (1998) was adapted to solve Equations (1-3) for shear thinning fluids. The diffusion time step limitation in the explicit Rudman algorithm was eliminated using the semi-implicit time stepping procedure of Li and Renardy (2000) to facilitate the calculation of very low Reynolds number flows. Axi-symmetric flow calculations were performed in cylindrical polar coordinates on the symmetric half of the computational domain (radius $4a$). A uniform grid with 16 cells spanning a nozzle inner radius (a) was chosen. Doubling the mesh density had a negligible effect on the predicted drop evolution in test cases.

RESULTS

Predicted drop shapes for a Newtonian drop are compared with corresponding photographic images as reported by Davidson et al. (2003) and are shown here in Figure 2. In that case Re = 1.25, We = 0.000687 and Fr = 0.00437. The results show that the overall detail of the drop shape, including the neck and the satellite drop formation, is closely predicted. See Davidson et al. (2003) for further details. Results for shear-thinning fluids are presented below for varying Ohnesorge number Oh = $\mathrm{We}^{1/2}/\mathrm{Re}$ based on the zero shear viscosity. The Ohnesorge number represents a ratio of viscous to surface forces. For the Newtonian case in Figure 2, Oh = 0.021.

The calculations in Davidson et al. (2003) were performed without including the region inside the nozzle (height $2a$ in Figure 1) in the computational domain. Including the nozzle region proved to have a negligible effect for large enough liquid viscosity (Oh > 0.02 with We and Fr fixed at the values above), which is true for the cases considered by Davidson et al. (2003). However, it is important to include this region for lower viscosity liquids as will now be explained. As the neck thins, liquid flows out of it by exiting downwards from the bottom and upwards from the top of the neck (Wilkes et al., 1999). Decreasing the viscosity reduces the normal viscous stresses resulting in an increase in the pressure in the neck which, in turn, increases the velocity of outflow from the neck. The upwards flow out of the neck collides with the liquid flowing down through the nozzle opening, creating a stagnation point. The location of the stagnation point depends on the velocity of the reverse upward flow

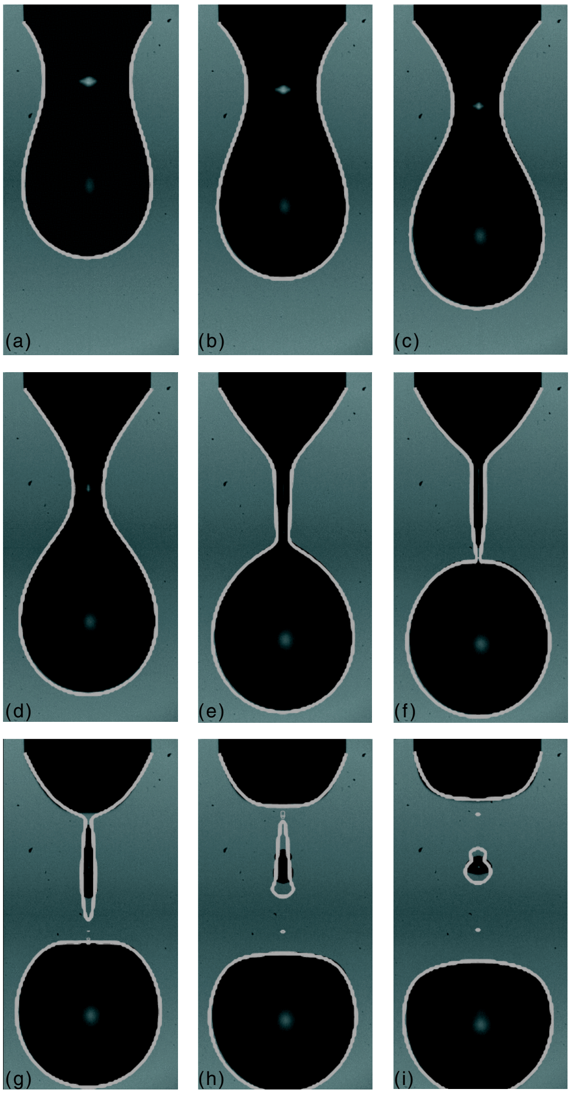

Figure 2: Predicted drop shapes (white outlines) compared with corresponding photographic images from an experiment for a Newtonian liquid. The sequence (a-i) corresponds to —30, -20, -10,-5, -1, 0, 1, 2, 3 milli-seconds, respectively, from the moment of pinch-off.

(and hence on the liquid viscosity). For Newtonian fluids, Wilkes et al. (1999) showed that this stagnation point penetrates the region inside the nozzle if the viscosity is low enough. In such cases a region inside the nozzle must be included in the computation domain.

Figure 3 shows the effect on minimum neck width (h) of decreasing either the zero shear viscosity (decreasing Oh) or the infinite shear viscosity (decreasing η_∞), while keeping the other fixed. Changes in η_∞ represent changes in the degree of shear-thinning. The overall effect is a more rapid narrowing of the neck. However, the neck width h is predicted to be insensitive to shear-thinning when Oh = 0.2. The reason for this is not known. The overall effect of varying Oh and η_∞ is consistent with predictions of the effect of viscosity on Newtonian pendant drops (Wilkes et al., 1999).

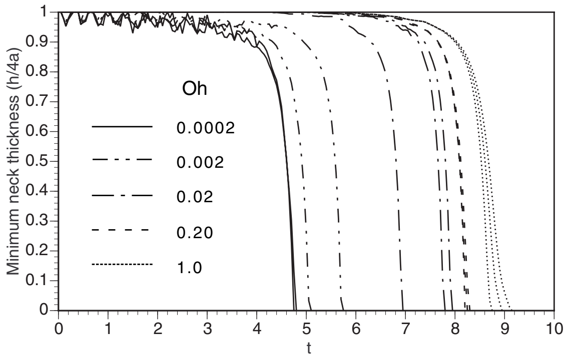

Figure 3: Minimum neck thickness for Newtonian ($\eta_\infty = 1.0$) and shear-thinning liquids ($\eta_\infty = 0.2, 0.6$) for different values of Oh when We = 0.000687 and Fr = 0.00437. Results for $\eta_\infty = 0.6$ are not shown for Oh < 0.02. Other shear-thinning parameters are $\lambda = 1$ and n = 0.2. The curves shift to the right with increasing η_∞ for each Oh value.

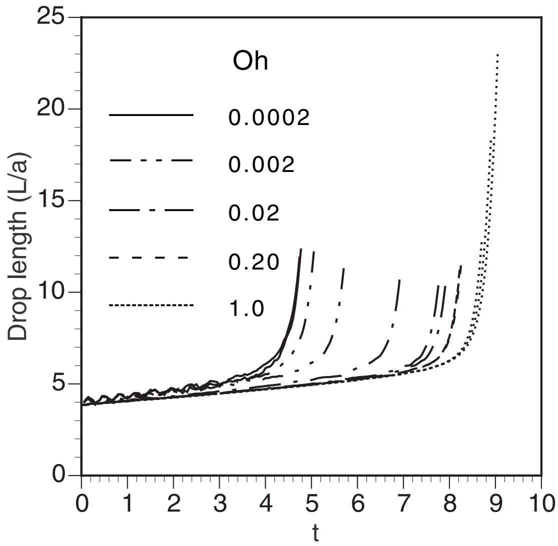

Figure 4: Drop length below the nozzle for Newtonian and shear-thinning liquids for the cases shown in Figure 3. For each Oh value, the curves shift to the right with increasing η_∞.

The dependence of drop length L prior to pinch-off on Oh and η_∞ is shown in Figure 4. In each case, L is seen to grow slowly at first, followed by a very rapid increase, as expected. This rapid increase occurs sooner as either Oh or η_∞ decreases, except when the viscosity is very small (small Oh). The limiting length achieved is predicted to have a minimum with respect to Oh. For the largest Oh values, the limiting length increases with Oh because the neck drains more slowly as viscosity increases. However for Oh < 0.02, instead of continuing to decrease, the limiting length increases as Oh decreases (at least until Oh = 0.0002 at which further reductions in viscosity have no effect). This occurs because, although the more rapid thinning of the neck as the viscosity (and hence Oh) decreases promotes a shorter limiting length, the velocity of liquid expelled from the neck increases sufficiently for the drop below the neck to assume an ellipsoidal shape with its long axis in the direction of flow; this tends to increase L.

The net effect of these two opposing trends is to increase L as Oh decreases from 0.02 to 0.0002. The effect of changing η_∞ follows the same trend as for changing Oh.

At the smallest zero shear viscosity (Oh = 0.0002) in Figures 3 and 4, both h and L are insensitive to shear-thinning. This occurs because changes in a viscosity which is already very small will have little effect. This has been noted by Yildirim and Basaran (2001) in relation to non-Newtonian liquid bridges. The oscillations in h and L which are predicted to develop initially as the zero shear viscosity is reduced (decreasing Oh) occur because of the impulsive start to the flow. The oscillations are damped out if the viscosity is large enough. Such oscillations have been found in low viscosity calculations of Newtonian drop formation (Wilkes et al., 1999).

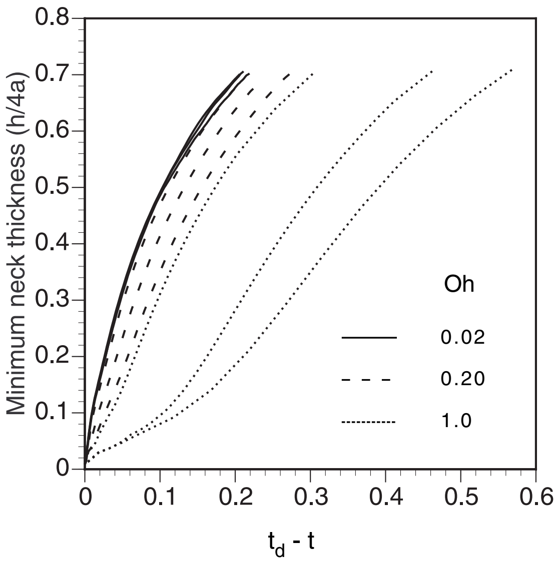

Figure 5: Minimum neck thickness, as a function of time measured backwards from the time of from pinch-off, for Newtonian ($\eta_\infty = 1.0$) and shear-thinning liquids ($\eta_\infty = 0.2, 0.6$). For each Oh value, the curves shift to the right with increasing η_∞. Other parameters are the same as for Figure 3.

Figure 5 shows the variation of h near pinch-off in more detail as a function of time measured backwards from the time of pinch-off (t_d). Here t_d is chosen to be the time at which $h/4a = 0.01$ which is approximately equal to the resolution of the grid. For Oh = 1, the viscosity is greatest and so is the effect of shear thinning (η_∞) on the h variation. As the infinite shear viscosity decreases, the rate of variation in h increases. For decreasing viscosity (reducing Oh), the effect of shear thinning reduces until Oh = 0.02 whereupon the time dependence of h, relative to the moment of pinch off, falls on a common curve. This limiting, low viscosity curve exhibits a $(t_d - t)^{2/3}$ time dependence which accords with the scaling law for potential flow. However, the numerical resolution is too coarse to predict the transition to a linear time dependence which occurs when h becomes of order Oh^2 and the viscosity of the surrounding air becomes important (Lister and Stone, 1998, Chen, Notz and Basaran, 2002).

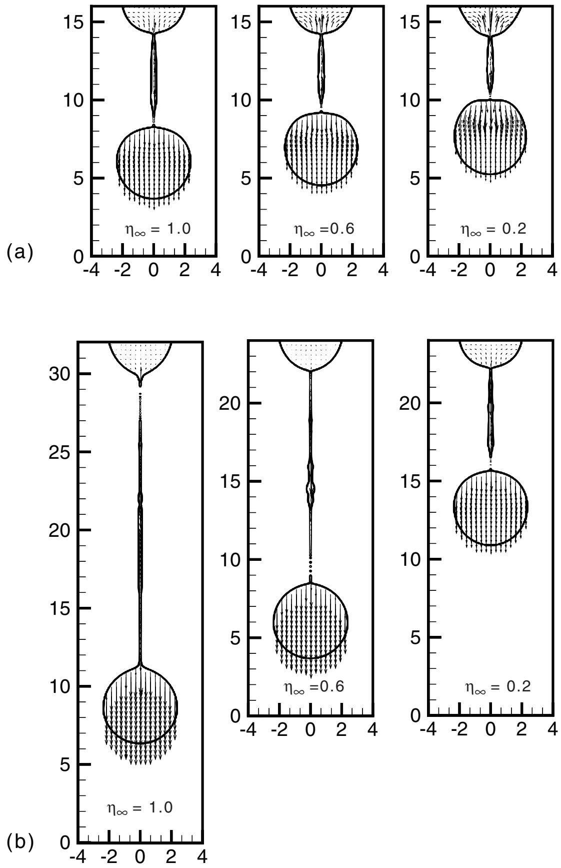

Figure 6: Predicted drop shapes and liquid velocity vectors near the moment of pinch-off for Newtonian ($\eta_\infty = 1.0$) and shear-thinning liquids ($\eta_\infty = 0.2, 0.6$) when (a) Oh = 0.2 and (b) Oh = 1.0. Other parameters are the same as for Figure 3.

Figure 6 shows the final drop shapes predicted at pinch-off when Oh = 0.2 and 1.0. Both cases show a reduction in final neck length due to shear-thinning, consistent with Figure 4 for these Oh values. The effect is greater for the higher the initial viscosity (Oh = 1.0) because the subsequent change in viscosity with shear rate is then greater for given $\eta_\infty < 1$. The velocity vectors for Oh = 0.2 show the outflow at the top and bottom of the neck. The outflow at the top of the neck (which opposes the downward flow from the nozzle) is seen to increase with shear-thinning (decreasing η_∞). This occurs for the same reason that the neck drains more rapidly, as discussed by Wilkes et al. (1999) for Newtonian drops.

An instability in the filament for Oh = 1.0 (Figure 6b) is evident by the bumps along its length. This is similar to the instability described for highly viscous jets close to break-up (Eggers, 1997). Interestingly, the neck is predicted to break first at the top for the Newtonian case (highest overall viscosity), whereas in all other cases considered here, the break-up occurs first at the bottom. For the related problem of shear-thinning liquid bridges, Yildirim et al. (2001) found that pinch-off could occur from the top or the bottom of the neck, depending on the stretching speed.

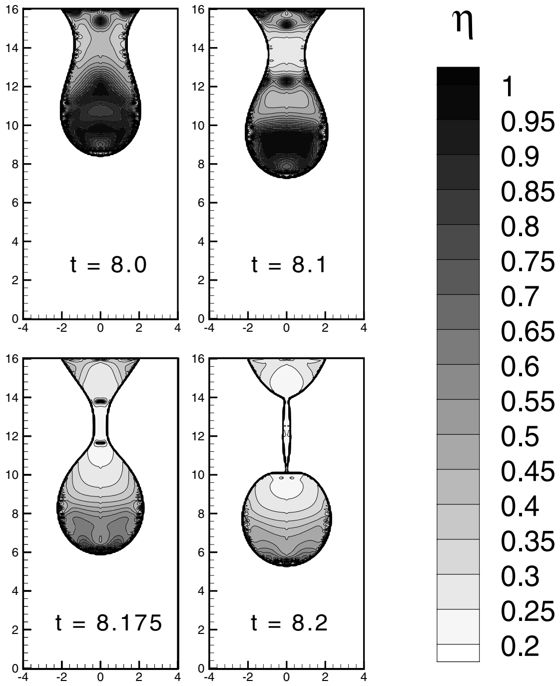

Figure 7: Predicted liquid viscosity contours during the approach to pinch-off for $\eta_\infty = 0.2$ and Oh = 0.2. Other parameters are the same as for Figure 3.

The variation of liquid viscosity in a shear-thinning drop at selected times during the approach to pinch-off is shown in Figure 7 for $\eta_\infty = 0.2$ and Oh = 0.2. Initially the liquid viscosity equals its value at zero shear rate ($\eta = 1$). As the drop begins to neck the viscosity in the neck begins to fall in response to the increased shear rate in that region. As the neck continues to thin, the region of lower viscosity grows to encompass almost the entire drop with the lowest values ($\eta = \eta_\infty$) occurring within the neck and just outside it where the outflows from the neck occur.

CONCLUSION

The evolution of a drop of shear-thinning liquid forming at a nozzle, directed vertically downwards in air, is predicted using a Volume-of-Fluid numerical method. The paper forms part of an on-going study. The effect of shear-thinning is a more rapid reduction in the thickness of neck analogous to the effect of reducing the viscosity of a Newtonian drop. For the values of Weber number and Froude number chosen, the limiting length of the drop prior to pinch-off exhibits a minimum as the zero-shear viscosity is varied. Predictions for a high viscosity drop show instabilities along the neck as it forms into a thin filament. The increase in the limiting drop length with reducing shear thinning at high viscosity is shown.

REFERENCES

AMAROUCHENE, Y., BONN, D., MEUNIER, J. and KELLAY, H., (2001), Inhibition of the finite-time singularity during droplet fission of a polymeric fluid , *Phys. Rev. Lett.*, **86**(16)**,** 3558-3561.

AMBRAVANESWARAN, B. WILKES, E.D. and BASARAN, O.A., (2002), Drop formation from a capillary tube: Comparison of one-dimensional and two-dimensional analyses and occurrence of satellite drops , *Phys. Fluids*, **14**(8)**,** 2606-2621.

BIRD, R.B., ARMSTRONG, R.C. and HASSAGER, O., (1987), *Dynamics of Polymeric Liquids* , Volume 1, 2nd edition, John Wiley & Sons, p. 171.

CHEN, A.U., NOTZ, P.K. and BASARAN, O.A., (2002), Computational and experimental analysis of pinch-off and scaling , *Phys. Rev. Lett.*, **88**(17)**,** art. No 174501.

COOPER-WHITE, J.J., FAGAN, J.E.,TIRTAATMADJA, V., LESTER, D.R. and BOGER, D.V., (2002), Drop formation dynamics of constant low viscosity, elastic fluids , *J.Non-Newt, Fluid Mech.*, **106,** 29-59.

DAVIDSON, M.R., COOPER-WHITE, J.J. and TIRTAATMADJA, V., (2003), Shear-thinning drop formation , *Computational Techniques and Applications Conference CTAC2003*, Sydney, Australia, July 7-9, 2003.

EGGERS, J., (1997), Nonlinear dynamics and breakup of free-surface flows , *Rev. Modern Phys.*, **69**(3)**,** 865-929.

GUEYFFIER, D., LI, J., NADIM, A., SCARDOVELLI, R. and ZALESKI, S., (1999), Volume-of-fluid interface tracking with smoothed surface stress methods for three-dimensional flows , *J. Comp. Phys.*, **52,** 423-456.

LI, J. and RENARDY, Y., (2000), Numerical study of flows of two immiscible liquids at low Reynolds number , *SIAM Review,* **42**(3)**,** 417-439.

LISTER, J.R. and STONE, H.A., (1998), Capillary breakup of a viscous thread surrounded by another viscous fluid , *Phys. Fluids*, **10**(11)**,** 2758-2764.

NOTZ, P.K., CHEN, A.U. and BASARAN, O.A., (2001), Satellite drops: Unexpected dynamics and change of scaling during pinch-off , *Phys. Fluids*, **13**(3)**,** 549-552.

RUDMAN, M., (1998), A volume tracking method for interfacial flows with large density variations , *Int. J. Numer. Meth. Fluids*, **28,** 357-378.

WILKES, E.D., PHILLIPS, S.D. and BASARAN, O.A., (1999), Computational and experimental analysis of dynamics of drop formation , *Phys. Fluids*, **11**(12)**,** 3577-3598.

YILDIRIM, O.E. and BASARAN, O.A., (2001), Deformation and breakup of stretching bridges of Newtonian and shear-thinning liquids: comparison of one and two-dimensional models , *Chem. Eng. Sci.,* **56,** 211-233.

ZHANG, D.F. and STONE, H.A., (1997), Drop formation in viscous flows at a vertical tube , *Phys. Fluids,* **9**(8)**,** 2234-2242.

ZHANG, X., (1999a), Dynamics of drop formation in viscous flows , *Chem. Eng. Sci.,* **54,** 1759-1774.

ZHANG, X., (1999b), Dynamics of growth and breakup of viscous pendant drops into air , *J. Colloid Interface Sci.,* **212,** 107-122.